Assessing regional-scale variability in deforestation and forest degradation rates in a tropical biodiversity hotspot

Remote Sensing in Ecology and Conservation
Open Access
ZSL LET'S WORK FOR WILDLIFE

ORIGINAL RESEARCH

Assessing regional-scale variability in deforestation and forest degradation rates in a tropical biodiversity hotspot

Gabriel Yesuf[1,2], Kerry A. Brown[1] & Nigel Walford[1]

[1]Department of Geography and Geology, Kingston University, Surrey KT1 2EE, United Kingdom
[2]Lancaster Environment Centre, Lancaster University, Bailrigg LA1 4YQB, United Kingdom

Keywords
CLASlite, intensity analysis, land use and land cover change (LULCC), Madagascar, sub-pixel analysis

Correspondence
Department of Geography and Geology, School of Natural and Built Environment, Kingston University London, Penrhyn Road, Surrey, KT1 2EE, United Kingdom.
Tel: +44 208 417 2215;
E-mail: gabriel.yesuf@kingston.ac.uk

Funding information
This study was funded by Kingston University's Faculty Studentship.

Editor: Nathalie Pettorelli
Associate Editor: Martin Wegmann

Received: 16 September 2018; Revised: 25 January 2019; Accepted: 30 January 2019

doi: 10.1002/rse2.110

Remote Sensing in Ecology and Conservation 2019;**5** (4):346–359

Abstract

Deforestation and forest degradation are major drivers of global environmental change and tropical forests are subjected to unprecedented pressures from both. For most tropical zones, deforestation rates are averaged across entire countries, often without highlighting regional differentiation. There are also very few estimates of forest degradation, either averaged or localized for the tropics. We quantified regional and country-wide changes in deforestation and forest degradation rates for Madagascar from Landsat temporal data (in two intervals, 1994–2002 and 2002–2014). To our knowledge, this is the first country-wide estimate of forest degradation for Madagascar. We also performed an intensity analysis to categorize the magnitude and speed of transitions between forest, vegetation matrix, cultivated land and exposed surface. We found significant regional heterogeneity in deforestation and forest degradation. Deforestation rates decreased annually in lowland evergreen moist forest by −0.24% and in all other vegetation zones. Forest degradation rates had annual increases in the same period in lowland evergreen moist forest (0.09%), littoral forest (0.06%) but decreased in medium altitude moist evergreen forest (−0.25%), dry deciduous forest (−0.23%) and scelrophyllous woodland (−0.61%) in the same period. Despite these regional differences, higher rates of deforestation and forest degradation were consistently driven by rapid and large-sized conversions of largely intact forest to cultivated lands and exposed surfaces, most of which occurred between 1994 and 2002. These results suggest that while targeted conservation projects may have reduced forest degradation rates in some areas (e.g. medium altitude moist evergreen forest), the drivers of land cover change remain intense in relatively neglected regions. We advocate a more balanced approach to future conservation initiatives, one recognizing that deforestation and forest degradation, particularly in tropical Africa, are often driven by region-specific conditions and therefore require conservation policies tailored for local conditions.

Introduction

Tropical forests make up 52% of global forests (FAO, 2015). They also harbour two-thirds of the world's terrestrial biodiversity (Whitmore 1998) and 96% of the world's estimated tree species (Fine et al. 2009). Despite their global significance, these habitats are under unprecedented pressure from a variety of factors, including deforestation and forest degradation (Vieilledent et al. 2013). Deforestation involves anthropogenic large-scale forest clearance, while forest degradation mainly occurs from small-scale conversions of persistent and subtle thinning in forest cover, ultimately resulting in a landscape mosaic comprised of non-degraded, secondary and fragmented forests (Ghazoul et al. 2015). Both processes are usually accompanied by marked changes to forest structure, species composition and biodiversity (Achard et al. 2014; Barlow et al. 2016).

Although remote sensing techniques have enabled reliable detection and monitoring of deforestation in tropical

forests, the same has not been true for forest degradation (Berenguer et al. 2014). Whether natural, anthropogenic, landscape-scale or within-forest disturbances, quantifying tropical forest degradation has been historically challenging (Stibig et al. 2014; Barlow et al. 2016). The main obstacle is that estimating degradation requires identification of subtle changes in canopy cover occurring over small spatial scales, usually not readily available from remotely sensed data. However, it is becoming increasingly clear that reliable estimates of forest degradation in the tropics is vital, since the proportion of global forest affected by degradation is rising faster than areas impacted by deforestation (Herold et al. 2011; Berenguer et al. 2014).

Using proportions of net change in forest areas, such as those reported by the global forest resource assessments (e.g. FAO) masks differences at national-scales (Keenan et al. 2015). This is because tropical landscapes are often heterogenous and dependent on region-specific socio-economic dynamics, thus reporting single-values of forest loss may be misleading (Lambin et al. 2001). A disaggregated approach that highlights regional rates of deforestation and forest degradation is likely to reflect the nuanced differences in Sub-Saharan African (SSA) landscapes. Similarly, a disaggregated approach allows for an analysis of region-specific drivers of land use land cover change (LULCC) and estimates of their intensification (Scrieciu 2007). Despite the heterogeneous and region-specific nature of deforestation and degradation in tropical forests, many studies still give averaged estimates and few measure forest degradation.

Studies of land cover change are often biased towards forest loss (Achard et al. 2007; Hansen et al. 2010; Stibig et al. 2014), despite evidence that regenerating forests possess faster biomass recovery, higher productivity and carbon uptake compared to old-growth forests (Zahawi et al. 2015; Poorter et al. 2016; Mora et al. 2018). Moreover, recent studies indicate that forest regeneration may play a significant role in mitigating effects of climate change (Houghton et al. 2015; Chazdon et al. 2016; Phillips and Brienen 2017). Therefore, making forest gains a research priority can complement the core mandates of Reduced Emissions from Deforestation and Degradation (REDD) mechanisms, especially for SSA. The estimates of forest gains are rarely reported for the tropics, despite growing understanding of their role in forest change dynamics in the region (FAO, 2015). For SSA countries, a bias towards forest loss may negatively impact national strategies for achieving conservation targets including the robustness of LULCC assessments.

In Madagascar, reliable estimates of deforestation and forest degradation rates are affected by a dearth of unified baseline data on forest cover to reflect 20th century changes (Kull 2012). This has led to different estimates of deforestation and in some cases, contentious assessments of forest cover change (Mcconnell and Kull 2014; Aleman et al. 2017). Several studies have attempted to characterize changes taking place in Madagascan forests. Hansen et al. (2008) estimated the deforestation rates of <0.7% for tropical Africa including Madagascar; others have focused on structural characterization of littoral forests in the southeast (Ingram et al. 2005), patterns of forest patches and changes in dry deciduous forests (Zinner et al. 2014) or comparing the accuracy of different approaches in estimating forest cover losses (Grinand et al. 2013). Most of these studies utilize whole pixel image differencing to assess forest cover change, which does not account for the fine-scale processes caused by forest degradation (Harris et al. 2012). Still, Allnutt et al. (2013) apply sub-pixel analysis of deforestation and degradation within Masaola National Park in north-eastern Madagascar their result show significant losses in forest cover within 6 years, with minimal differences (±0.03%) between deforestation and forest degradation rates. Although Madagascar has submitted an updated 2018 Forest Reference Level (FREL) to the United Nations Framework Convention on Climate Change (UNFCCC), it only includes emission reductions from deforestation and does not include degradation, further highlighting the importance of assessing forest degradation in the country (United Nations Framework Convention on Climate Change (UNFCCC) 2018).

In this paper, we map deforestation and forest degradation rates for Madagascar using a sub-pixel analysis, which assessed changes in forest cover at ≤0.1 ha resolution. To our knowledge, there is no other assessment of localized forest changes caused by subtle, small-scale degradation across the island. Secondly, we investigate the impact of land-cover driven shifts in habitat types and analyse the intensity of land cover category transitions within habitats highly vulnerable to LULCC, yet slow to recover due to persistent disturbances. This disaggregated approach (i.e. analysing regions separately and combined) was adopted to highlight the regional differences in deforestation and forest degradation across the island, as they may be driven by distinct causes locally, or different biomes may respond differently to similar pressures. There is no *a priori* prediction about which regions would exhibit the highest or lowest rates of deforestation and forest degradation. However, the expectation is for shifting cultivation to be an active driver in all regions, while increases in exposed surfaces, possibly caused by erosion and/or wildfires to actively degrade arid forests (Carter et al. 2018). Next, we also account for forest regeneration in our analysis to provide a complete picture of forest change dynamics (Hansen et al. 2013). We do not present a conceptual distinction between the processes leading to

forest gain, including forestation, afforestation or reforestation. Rather, intensity analysis is utilized to detect land cover category swaps to forest, as well as all other transitions taking place in two intervals (see below).

Materials and Methods

Study area: geographical setting of eco-regions

Madagascar is the fourth largest island in the world and forms the major portion of one of 34 global biodiversity hotspots, characterized by high floral and faunal endemism, as well as threats from deforestation and degradation. In this paper, land use land cover change assessment is implemented for dominant vegetation zones as defined in Gautier et al. (2018). These vegetation zones are littoral forest, lowland evergreen moist forest, medium altitude moist evergreen forest, dry deciduous forest and sclerophyllous woodland (Fig. 1). The highly degraded and fragmented montane forests and spiny thickets were excluded because they are not strictly forested regions. Mangroves were also excluded because they face different pressures and impacts which are not present in other vegetation zones. We define forested areas as portion of the landscape with greater than 25% closed canopy cover, covering an area more than 0.5 ha largely made up of trees whose height exceeds 5 m and the predominant absence of other land-uses (FRA, 2000; Hansen et al. 2010).

The littoral forest is situated on the eastern border of the island close to sea level on sandy sediments rising to an elevation of 100 masl (metres above sea level) in some areas (Insets in Fig. 1). Due to low elevation and subsequent easy accessibility, littoral forests are under constant pressure and are now regarded as the country's most threatened vegetation zone and is predicted to disappear unless drastic measures are taken (Crowley 2010; Andriamandimbiarisoa et al. 2015). The lowland evergreen moist forest constitutes the region that mostly borders the Indian Ocean to the east in a northerly and southerly direction, at an elevation range of 0–800 masl covering an area of *c.* 30 000 km^2. Following a similar orientation is the medium altitude moist evergreen forest which range in elevation from 800 to 1800 masl occupying an area of *c.* 34 000 km^2. The dry deciduous forest occurs along the western axis and also in the extreme north, bordering the Mozambique channel in some parts with an elevation range of 0–800 masl and covers *c.* 24 000 km^2 of land area (Gautier et al. 2018). The scelrophyllous woodland elevation ranges from 800–1800 masl dissecting parts of the montane forests and in large patches along the southwest region (Fig. 1) covering an area of *c.* 1470 km^2 (Kull 2002a; Rakotondrasoa et al. 2012).

Selection of satellite imagery

The following imagery was used for LULCC assessment: Landsat Thematic Mapper (TM), Enhanced Thematic Mapper plus (ETM$^+$) and Operational Land Imager (OLI). All datasets were obtained from the archives of United States GloVis viewer and had a 30-m spatial resolution (http://glovis.usgs.gov/) (Table S1). The satellite images collected enabled repetitive measurements of land cover change covering 20 years in three image time stamps. The first time stamp comprised of Landsat TM images from predominately 1994, but also included 1995 and 1996. The second time stamp comprised of Landsat ETM$^+$ images from 2000, 2001 and predominantly 2002. The third time stamp included Landsat OLI images from 2013 and predominately 2014. For each time stamp, images were selected based on the date of image acquisition (late dry to early rainy season) and the absence of cloud cover (<10%). The analyses were carried out using two intervals: the first interval consisted of images from *c.* 1994 to *c.* 2002; while the second interval was defined by images from *c.* 2002 to *c.* 2014. All Landsat imagery was Level 1T, which had been processed for radiometric calibration and geometric correction using digital elevation models of terrestrial surface of Madagascar (Lee et al. 2004).

Assessing rates of deforestation and forest degradation

The proportion of deforestation and forest degradation in each interval was estimated using CLASlite v3.3 (http://claslite.carnegiescience.edu/en/about/software.html), which allows for mapping forest cover change at large scales and can detect forest degradation occurring at less than a hectare (Asner et al. 2009). The analysis required the use of forest cover obtained from Landsat imagery to analyse sub-spectral characteristics of pixels across Madagascar (Martínez et al. 2006; Asner et al. 2009). The images were corrected for radiometric errors caused by atmospheric attenuation using rescaled gains and bias (offsets) parameters provided for each band. These rescaled values underwent a second simulation (6S transfer model) that resolved errors untreated during the initial rescaling process, before the radiance values were converted to surface reflectance values (Vermote et al. 1997). The simulation model used NASA's MODIS data in the background to modulate the effect of the atmosphere on sun rays as it interacts with the atmosphere and land surface. The raw Landsat imagery input was then corrected by removing the estimated model of the atmosphere, leaving an image of the resultant surface reflectance (0–100%). Thereafter, each image scene was examined to determine the suitable

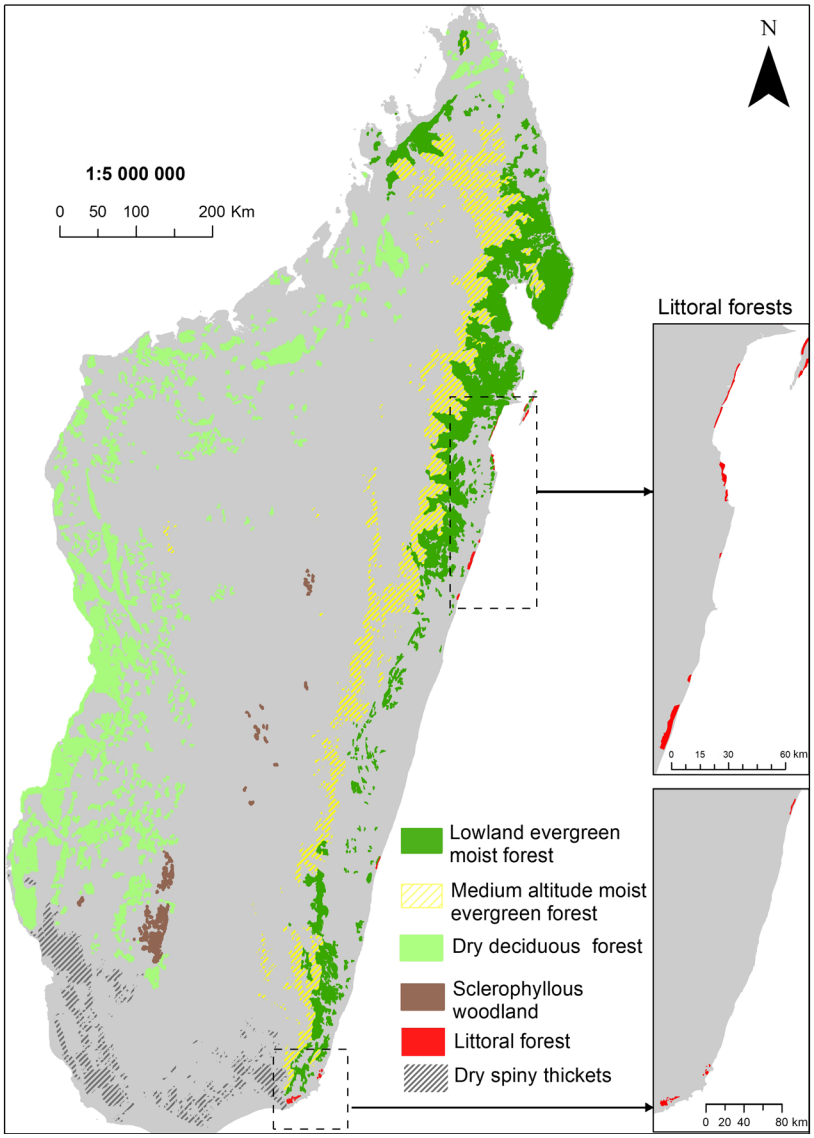

Figure 1. Selected vegetation zones of Madagascar showing forested areas. Forested areas were characterized by >25% closed canopy cover with trees taller than 5 m. Insets are littoral forests on the eastern coast of the Island. Vegetation zone shapefiles downloaded from Royal Botanic Gardens, Kew website and cartographic visualization implemented in GIS. Vegetation zones following the classifications of Gautier et al. 2018. *Map projection: Geographic coordinate system using WGS1984 datum.*

threshold to set the mask for water, clouds and shadow (reduced masking approach); this was done to avoid over-masking, especially in areas of high relief. Next, the composition of each pixel fraction was determined using Auto Monte Carlo pixel-Unmixing (AutoMCU) (Quintano et al. 2012), a probabilistic algorithm that takes each input pixel reflectance value and decomposes it into three component fractions: live vegetation, dead vegetation and bare substrate.

During the process of pixel decomposition, each fraction component was compared with historical modelled values in CLASlite's spectral libraries. These spectral libraries consisted of large collections of representative samples of individual components corresponding to pure spectra for each of the land cover components (i.e. spectral end-members). The end-member libraries in CLASlite are available for tropical regions only. They consist of detailed signatures of bare substrate and dead vegetation ground-truthed using field observation. Live vegetation signatures were collected from airborne hyperspectral sensors due to the impediments associated with tropical forest landscapes usually in the form of large crowns and

basal areas. Previous studies have demonstrated the effectiveness of AutoMCU in mapping tropical ecosystems, including savanna, woodland, shrubland and broadleaf forests (Asner et al. 2005; Allnutt et al. 2013). Next, the pixel values were analysed using decision trees, where splits were based on the analyses of differences between pixel components at the start and end of intervals. The differences in the proportion of these components from 1994 to 2014 were used to determine deforested and degraded pixels. Generally, the reductions in live vegetation within pixels that were ≥60% represented deforested pixels, while those ≥40% suggested forest degradation (Asner et al. 2009).

The process of decomposition required identification of the optimum threshold for which a pixel's component could be quantified into different fractions. In moist ecoregions (i.e. littoral, medium altitude moist evergreen and lowland evergreen moist forests) live vegetation components were predictably higher for most pixels (average 90%), 5% for dead vegetation components and negligible values for bare substrate. Whereas in western dry forests, live vegetation component values were comparably lower than those of medium altitude moist evergreen forests, averaging 80% per pixel, while dead vegetation and bare substrate values were on average around 15% and 5% respectively. In the scelrophyllous woodland, there was very wide variation in all three component values measured during pixel unmixing. Therefore, a 50% optimum threshold was selected for decomposition. For each interval, the sizes of deforested and degraded area were determined in GIS and represented the portion of the pixels whose live vegetation fraction was below 60% and 40%. The rates of deforestation and degradation were calculated and Mann–Whitney *U*-test was performed to compare whether there were any differences between deforested and degraded area sizes between intervals (i.e. 1994–2002 and 2002–2014).

Mapping land use land cover change

Following the classification scheme of Moat and Smith (2007) for Madagascar, thematic land use classes were identified in each vegetation zone. Moat and Smith (2007) classification was modified to form four distinct classes: forest, vegetation matrix (includes grassland, wooded grassland and highly degraded forest), cultivated land and exposed surface (includes urban areas). These land use classes served as an implicit measure of the drivers of deforestation and forest degradation (Paneque-Gálvez et al. 2013; Haque and Basak 2017). Training sites were identified randomly with the aid of high resolution Quick Bird images (Google Earth) in ERDAS Imagine (Vieilledent et al. 2013; Devries et al. 2015), as well as sites selected from multiple land cover categories directly observed by Brown et al. (2013) during their field research in Madagascar. Images were classified into land use land cover maps using the maximum likelihood technique which was implemented for each time stamp imagery. The derived maps were cross-tabulated to obtain a square contingency table of land cover transitions to determine three-pixel states in each interval: (1) persistence; (2) gains and (3) losses. Thereafter, the intensity analysis was implemented to determine the causes of land cover transitions and to partition the speed and magnitude of these transitions into two time intervals (e.g. *c.* 1994–2002 and *c.* 2002–2014) (Aldwaik and Pontius 2012). Two component parts of the intensity analysis (i.e. observed and uniform intensities) were quantified. In each interval, uniform intensity for each observed intensity transition was estimated to explain differences in the rate of change and how these differences affected gross gains or losses. The estimated rates represent measures of speed of category transitions. Furthermore, the annual observed transition intensity for different land cover category swaps relative to the speed of other transitions taking place in each interval was quantified. The observed transition intensities were aggregated to determine the magnitude of land cover category swaps and their intensity of gains and losses in each interval. Gains were determined relative to magnitudes of LULCC categories in the initial year and losses relative to the magnitudes in the subsequent year for each category swap in each interval.

Transitions from forest pixels to all non-forest state pixels (i.e. vegetation matrix, cultivated land, exposed surfaces) were used as implicit measures for estimating drivers of deforestation and forest degradation. Likewise, transitions from vegetation matrix to exposed surface and cultivated land, as well as all transitions from cultivated land to exposed surface were considered as drivers for both deforestation and forest degradation. Similarly, transitions from exposed surface and cultivated land to forest and vegetation matrix were also quantified. These categorizations allowed assessment of how the magnitude, speed and nature of transitions vary between vegetation zones over 20 years.

Validating patterns of LULCC

Quantifying errors in sub-pixel analysis

The uncertainties associated with the results of deforestation and forest degradation rates were quantified using a combination of standard deviation and root mean square error (RMSE). The root mean square error compared the difference between predicted end-member values for the region and measured end-member values quantified from

the input images. Both the standard deviation (results not presented) and RMSE of the modelled results allowed for the assessment of the uncertainty associated with the derived rates of deforestation and forest degradation. Furthermore, we compare the results obtained from our analysis with Hansen et al. (2013) global forest change datasets to determine the extent of agreement between the areas of forest loss (Fig. S2).

Accuracy assessment of land cover maps

Reference pixels were independent of the training samples used during image classifications and were assessed against randomly selected verification datasets. The verification datasets consisted of 250 locations randomly selected across the island using Google Earth high resolution images. To account for bias in sampling intensity commonly associated with land cover category sizes, the different measures of accuracy were weighted against the proportion of the categories in each map (Olofsson et al. 2014). Using error matrices, the number of reference (sample) pixels assigned to different land cover categories were determined relative to the verified datasets collected from Google Earth. Then, accuracy of the classifications was calculated and expressed as three metrics: overall accuracy (OA), user's accuracy (UA) and producer's accuracy (PA). The OA for each classification was derived by dividing the number of total correct (diagonal) by the total number of pixels in the error matrix. The PA determines the probability of correctly classifying a reference pixel (i.e. error of omission) obtained by dividing the total number of correct pixels of any given category by the total number of pixels of that category in the reference data. UA provides the probability that a pixel classified on the map corresponds to the same category in the verification data (i.e. error of commission) and is calculated from the total number of correct pixels per category divided by the total number of pixels classified in that category (Tables S2–S3).

Results

Regional scale deforestation and degradation rates

Sub-pixel analysis showed that deforestation rates decreased in all vegetation zones, but forest degradation rates increased in lowland evergreen moist and littoral forests by 0.09% $year^{-1}$ and 0.06% $year^{-1}$ (Table 1). Sclerophyllous woodland had the lowest deforestation (-0.87% $year^{-1}$) and forest degradation (-0.61% $year^{-1}$) rates. In littoral forest, high forest degradation rates did not equally translate to high deforestation rates. The deforestation rates in dry deciduous forest were much lower than forest degradation rates in the same period. Minimal differences between deforestation and forest degradation was detected in medium altitude evergreen forest (Table 1). The accuracy associated with deforestation and forest degradation results were mapped and show variations in error for each time stamp (Fig. S1).

Comparing sizes of deforestation and forest degradation by intervals

Interval comparisons revealed that there was significant difference between the sizes of deforested areas in medium altitude moist evergreen forest, dry deciduous forest and sclerophyllous woodland (Mann–Whitney *U*-test, $P<0.001$; Table 2). During the second interval (i.e. 2002–2014), large-sized deforestation was dominant in medium altitude moist evergreen forest and dry deciduous forest which suggest an increase in the severity of deforestation in these vegetation zones (Fig. 2).

There were significant differences in sizes of forest degradation during first (i.e. 1994–2002) and second interval in all vegetation zones. For instance, in littoral forests, forest degradation sizes were significantly smaller in the first interval compared to the second interval (Mann–Whitney *U*-test, $p<0.001$; Table 2). Similarly, the average area of degradation was smaller in the first interval than in the second interval in medium altitude moist evergreen and dry deciduous forests. Generally high deforestation and degradation rates did not always translate to the presence of large-sized forest clearings within vegetation zones. For instance, on average deforested area sizes in dry deciduous forests were one of the largest during both intervals (Fig. 2) but relative to other zones had low deforestation rates (Table 1). Areas of agreement between sub-pixel analysis and the global forest change dataset by Hansen et al. (2013) for Madagascar reveal considerable agreement between both maps (Fig. S2).

Forest loss vs. forest gains

Forest loss out-stripped forest gain in littoral and dry deciduous forests. However, the proportion of forest gained was larger than deforestation and degradation in both intervals for lowland evergreen moist and medium altitude moist evergreen forests (Table 3). In littoral forest, the proportion of forest gains (1.2%) was smaller than those of forest loss (3.5%). Although during second interval, the proportion of forest gains was larger than losses due to deforestation and degradation. A similar pattern was detected in dry deciduous forest where combined forest losses impacted 6.4% of the landscape compared to 0.5% of areas experiencing forest gains.

Table 1. Summary of deforestation and forest degradation rates as quantified from sub-pixel analysis for selected vegetation zones of Madagascar. Rates in each vegetation zone are listed in descending order for both deforestation and forest degradation.

	Deforestation (ha)				Degradation (ha)		
Vegetation Zones	1994–2002	2002–2014	RoC (%year^{-1})	Vegetation Zones	1994–2002	2002–2014	RoC (%year^{-1})
Lowland evergreen moist forest	149 706	123 708	−0.17	Lowland evergreen moist forest	42 938	46 702	0.09
Medium altitude moist evergreen forest	130 889	99 525	−0.24	Littoral forest	135	143	0.06
Dry deciduous forest	222 040	135 577	−0.39	Dry deciduous forest	22 775	17 602	−0.23
Littoral forest	859	341	−0.60	Medium altitude moist evergreen forest	43 305	32 457	−0.25
Sclerophyllous woodland	7353	961	−0.87	Sclerophyllous woodland	2142	834	−0.61

Table 2. Comparative analysis of mean sizes of deforestation (def.) and forest degradation (deg.) categorized by intervals for selected vegetation zones of Madagascar. Statistically significant results between intervals are highlighted in bold (α=0.05).

Vegetation zone	Interval	Mean def. area (ha)	Sig.	Mean deg. area (ha)	Sig.
Medium altitude moist evergreen forests	1994–2002	0.69	**<0.001**	0.17	**<0.001**
	2002–2014	0.82		0.20	
Lowland evergreen moist forests	1994–2002	0.69	0.87	0.18	**<0.001**
	2002–2014	0.70		0.19	
Littoral forests	1994–2002	0.93	0.86	0.15	**<0.003**
	2002–2014	0.63		0.19	
Dry deciduous forests	1994–2002	1.45	**<0.001**	0.17	**<0.001**
	2002–2014	1.52		0.20	
Sclerophyllous woodland	1994–2002	0.52	**0.002**	0.16	**0.01**
	2002–2014	0.48		0.15	

Sig. represents the significance of Mann–Whitney *U*-test between intervals for each vegetation zone.

Magnitude and nature of land use land cover transitions

Quantifying forest loss and other transitions

Largely, forest transitions to exposed surface and vegetation matrix, as well as vegetation matrix transitions to exposed surface and cultivated land were on average faster and larger than other transitions and mainly occurred in the first interval (Fig. 3A–E). Specifically, large and relatively fast transitions from forest and vegetation matrix to cultivated land and/or exposed surface dominated transitions in the lowland evergreen moist, medium altitude moist evergreen and dry deciduous forests. Sclerophyllous woodland was dominated by large transitions of cultivated land to exposed surface in the second interval. However, the fastest transitions were of forest to exposed surface, albeit at a lower magnitude (Fig. 3D). In the second interval, fewer large-sized transitions occurred in medium altitude moist evergreen forests, compared to the lowland evergreen moist forests where more intermediate- to small-sized transitions of forest to cultivated land and vegetation matrix to cultivated land were detected. On average, second interval transitions in four of the five eco-regions were slower than first interval transitions regardless of the type of transitions. Only within the littoral forests did this pattern differ, with almost identical speeds between large-sized transitions of forest to cultivated land.

All observed transitions from the perspective of forest loss during the first and second intervals were mapped and provided as Figs. S3–S5. The overall accuracy of the *c.* 2014 land cover maps was 84% and higher than that of *c.* 2002 maps at 74%. The associated stratified producer and user accuracies are given in Tables S2 and S3.

Discussion

Quantified rates of deforestation and forest degradation

Our study documented significant regional differences in deforestation and degradation rates in Madagascar,

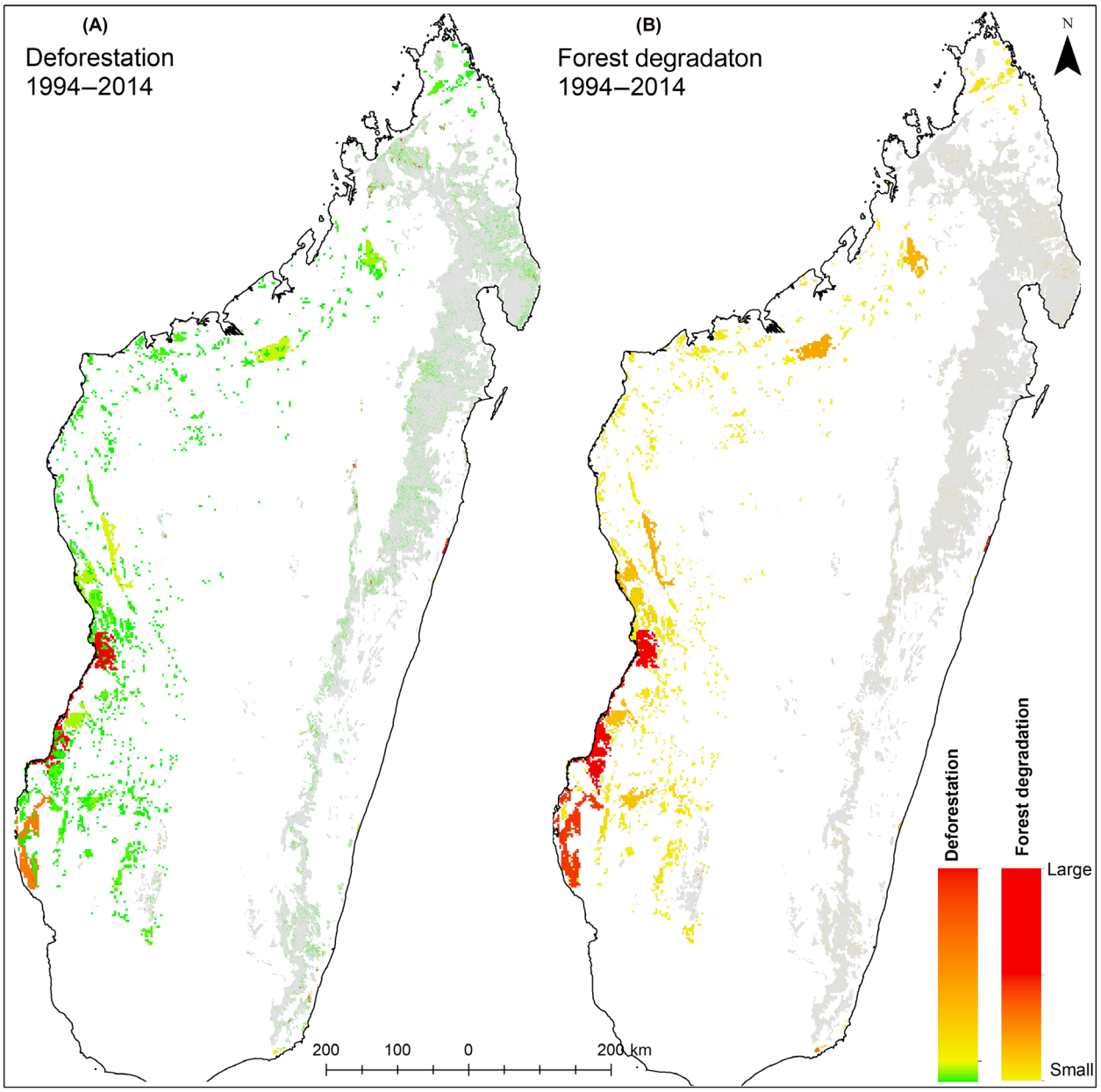

Figure 2. Outputs of sub-pixel analysis showing areas impacted by (A) deforestation and areas impacted by (B) forest degradation from 1994 to 2014.

highlighting the importance of partitioning the effects of LULCC at regional scales. Deforestation from lowland evergreen moist forest was the highest, though estimates for this study are lower than the most recent assessments for the region (Allnutt et al. 2013; Hansen et al. 2013). The deforestation rates for medium altitude moist evergreen and dry deciduous forests were considerably lower than estimates from Harper et al. (2008), (+0.8% year^{-1}) possibly because their assessment did not differentiate between deforestation and degradation within largely intact forests and perhaps due to an overestimation of deforested areas when using whole-pixel analytical techniques. Our assessment gives a nuanced view of deforestation rates across different regions of Madagascar, some of which align with recent studies that suggest a slowing of deforestation in unprotected tropical landscapes (Aleman et al. 2017). However, the magnitude of deforestation in Madagascan forests is likely to be more severe in the future, evidenced by the large-sized clearings detected in lowland evergreen moist, medium altitude moist

Table 3. Interval comparisons in the proportion of each vegetation zone affected by deforestation, forest degradation and forest gains.

	Lowland evergreen moist forest			Medium altitude moist evergreen forest			Littoral forest			Dry deciduous forest			Sclerophyllous woodland		
	1994–2002	%	2002–2014	1994–2002	%	2002–2014	1994–2002	%	2002–2014	1994–2002	%	2002–2014	1994–2002	%	2002–2014	%
Deforestation	149 706	4.9	123 708	130 889	3.9	99 525	859	3.1	341	222 040	9.3	135 577	7353	5.0	961	0.7
Forest degradation	42 938	1.4	46 702	43 305	1.3	32 457	135	0.5	143	22 775	0.9	17 602	2142	1.5	834	0.6
Forest gains	387 625	12.9	541 487	307 502	9.0	698 859	333	1.2	2519	22 573	0.9	12 232	11 490	7.8	15 940	10.8

Proportions were calculated relative to the sizes of each vegetation zone. Forest regeneration represents the transitions from vegetation matrix, cultivated land and exposed surface to forest.

evergreen and dry deciduous forests during the second interval. In western dry deciduous forests where natural habitats are relatively smaller, the average size of deforestation was the largest in both intervals compared to all other eco-regions. Such evidence of impact from deforestation in highly fragmented natural habitats reinforces the threats to all regions of Madagascar (Brown et al. 2015).

Moreover, these results also show early evidence that subtle thinning or within-forest disturbances is emerging as an active driver of change. However, there is no clear explanation for inconsistent forest degradation rates between regions. Though high forest degradation rates in lowland evergreen moist vegetation zones may be a consequence of the absence of large tracts of forests and the presence of small forest patches that are easily accessible (Eckert et al. 2011). Evidence of increased degradation rates supports recent studies showing that despite some successes in tackling deforestation in tropical regions, forest degradation may have evaded prior regulatory measures and poses a threat to largely primary forest habitats (Boucher et al. 2014; Barlow et al. 2016; Prestele et al. 2016).

The results of differences in regional deforestation and forest degradation rate highlight the complexity of change processes in Madagascan habitats. For example, shifting cultivation, selective logging and cyclones are major agents of forest cover change along the eastern escarpment, which comprises the lowland evergreen and medium altitude moist evergreen forests (Brown and Gurevitch 2004; Burivalova et al. 2015); while deforestation and degradation in dry forest are more likely modulated by shifting cultivation, livestock grazing, charcoal production and wildfires, and to a lesser degree, selective logging (Waeber et al. 2015; Feldt and Schlecht 2016). Consequently, although selective logging is often the most common cause of degradation in tropical forests (Asner et al. 2005), the influence of local drivers at the regional scales may differ or get displaced through leakages (i.e. spatial displacement in forest loss) (Gasparri et al. 2016). There are several explanations for these regional differences: one could be the consequence of pressures caused by in-migration of re-settlers to high elevation habitats (Devries et al. 2015). Alternatively, leakage may be driven by shifts in dryland cropping on slopes (*Tanety*) upland towards montane forests (Vågen 2006), seasonal burning (Kull 2002b) or slow reforestation of dry forests once exposed to disturbances (Zinner et al. 2014). Arguably, the dominant drivers of deforestation and forest degradation have shifted to other regions or are beginning to shift in an upslope direction. This may have led to increasing trends in deforestation and forest degradation in parts of Madagascar and decreasing trends in others.

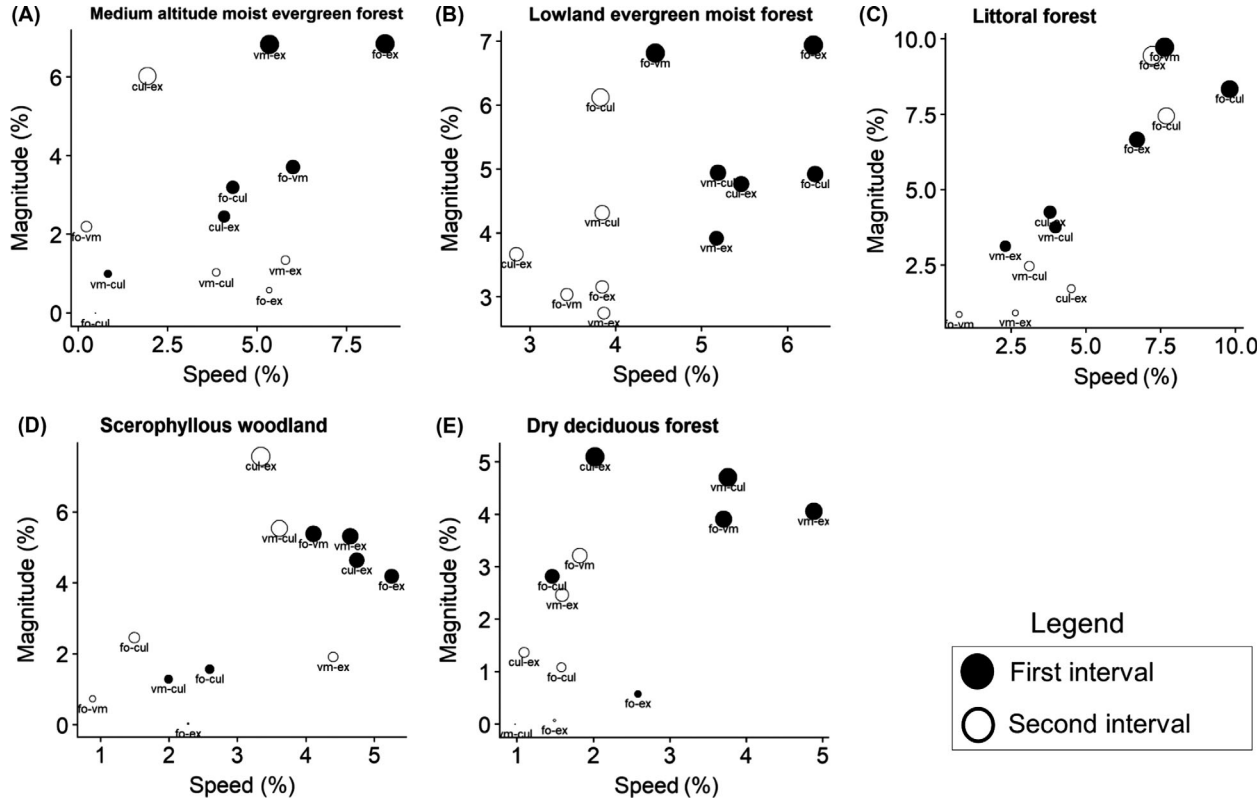

Figure 3. Difference between the nature of land cover category transitions in two intervals (*c.* 1994–2002 and *c.* 2002–2014) for five vegetation zones: (A) medium altitude moist evergreen forest; (B) lowland evergreen moist forest; (C) littoral forest; (D) scelrophyllous woodland; and (E) dry deciduous forest. Proportional bubbles depict large and small-sized transitions of land cover categories. Speed indicates the rate of change of land cover category swaps relative to other transitions taking place. First and second intervals transitions are depicted as black and white circles respectively. Note: *cul, cultivated land; ex, exposed surface; fo, forest; vm, vegetation matrix.*

Since these analyses did not explicitly estimate selective logging however, it was not possible to determine to what extent it modulates forest cover change. It should be noted that for the lowland evergreen moist forest, there was higher proportion of cloud cover in the *c.* 2002 imagery, which resulted in masking of those pixels during sub-pixel analysis and may be a contributing factor to the high rate of deforestation and verified with the error quantified for that vegetation zone.

Drivers of forest loss and other land cover transitions

The most frequent and largest magnitude transitions were from other categories to cultivated lands (during both intervals), confirming our expectation that shifting cultivation modulates land cover change in Madagascar (Elsa et al. 2017). It is worth noting that smaller-sized, slower transitions in the second interval do not necessarily reflect slowing deforestation and forest degradation. Instead, it may simply indicate that the process of degradation associated with transitions from cultivated lands to exposed surfaces is slower than converting largely intact forests to either of the other categories. Regions exhibiting increased deforestation and/or forest degradation had similarly large transitions to exposed surfaces, which suggests the presence of similar drivers of LULCC in both arid and moist forests (Zaehringer et al. 2015).

Conclusion

This study highlights considerable heterogeneity in rates of deforestation and degradation in Madagascar, with locally and regionally distinct patterns of both increasing and decreasing forest loss. Our study also suggests that although there were regional differences, increased rates of deforestation and degradation were consistently driven mainly by rapid and large-sized conversions of largely intact forest to cultivated lands. Similar trends could exist for other tropical regions but are often masked by rates of deforestation and degradation averaged across ecoregions and sometimes for entire countries. These results

and others (e.g. Waeber et al. 2015) suggest the adoption of a more balanced approach to future conservation initiatives, since deforestation and forest degradation are often driven by region-specific conditions and therefore require conservation policies tailored for local environments.

The detection of forest degradation in all vegetation zones highlights the value of the additional, often unreported contribution of degradation to forest cover change, the absence of which leads to continued underestimation of LULCC in the tropics. Perhaps this result could inform the ongoing debate surrounding the importance of quantifying and monitoring forest degradation in tropical developing countries. In regions where weak governance and insecure land tenure rights drive shifting cultivation, illegal selective logging and extraction of non-timber forest products – such as many countries in SSA – estimating forest degradation is equally as valuable as deforestation.

Acknowledgments

This study was funded by Kingston University's faculty studentship. We thank one anonymous reviewer and Steve Goodman for their comments on our initial submission, as well as Steig Johnson for his useful insights on this paper. We also thank KU's High-Performance Computing unit, especially Colin Bethell and Adam Hobbs for providing computing resources that enabled us to process our imagery and acknowledge the Carnegie CLASlite support team for providing the license and technical support. We have no conflict of interest to declare. The United States Geological Survey provided all Landsat images free of charge.

References

Achard, F., R. Defries, H. Eva, M. Hansen, P. Mayaux, and H. J. Stibig. 2007. pan-tropical monitoring of deforestation. *Environ. Res. Lett.* **2**, 045022.

Achard, F., R. Beuchle, P. Mayaux, H. J. Stibig, C. Bodart, A. Brink, et al. 2014. Determination of tropical deforestation rates and related carbon losses from 1990 to 2010. *Glob. Change Biol.* **20**, 2540–2554.

Aldwaik, S. Z., and R. G. Pontius. 2012. Intensity analysis to unify measurements of size and stationarity of land changes by interval, category, and transition. *Landsc. Urban Plan.* **106**, 103–114.

Aleman, J. C., M. A. Jarzyna, and A. C. Staver. 2017. Forest extent and deforestation in tropical Africa since 1900. *Nat. Ecol. Evol.* **2**, 26.

Allnutt, T. F., G. P. Asner, C. D. Golden, and G. V. Powell. 2013. Mapping recent deforestation and forest disturbance in northeastern Madagascar. *Trop. Conserv. Sci.* **6**, 1–15.

Andriamandimbiarisoa, L., T. S. Blanthorn, R. Ernest, J.-B. Ramanamanjato, F. Randriatafika, J. U. Ganzhorn, et al. 2015. Habitat corridor utilization by the gray mouse lemur, *Microcebus murinus*, in the littoral forest fragments of southeastern Madagascar. *Madagascar Conserv. Develop.* **10**, 144–150.

Asner, G. P., D. E. Knapp, E. N. Broadbent, P. J. C. Oliveira, M. Keller, and J. N. Silva. 2005. Selective logging in the Brazilian amazon. *Science* **310**, 480–482.

Asner, G. P., D. E. Knapp, A. Balaji, and G. Páez-Acosta. 2009. Automated mapping of tropical deforestation and forest degradation: CLASlite. *J. Appl. Remote Sens.* **3**, 033543.

Barlow, J., G. D. Lennox, J. Ferreira, E. Berenguer, A. C. Lees, R. M. Nally, et al. 2016. Anthropogenic disturbance in tropical forests can double biodiversity loss from deforestation. *Nature* **535**, 144–147.

Berenguer, E., J. Ferreira, T. A. Gardner, L. E. O. C. Aragão, P. B. de Camargo, C. E. Cerri, et al. 2014. A large-scale field assessment of carbon stocks in human-modified tropical forests. *Glob. Change Biol.* **20**, 3713–3726.

Boucher, D., P. Elias, J. Faires, and S. Smith. 2014. Deforestation success stories: tropical nations where forest protection and reforestation policies have worked. *Union of Concerned Scientists.* Available at https://www.ucsusa.org/forestsuccess. (accessed 18 August 2015).

Brown, K. A., and J. Gurevitch. 2004. Long-term impacts of logging on forest diversity in Madagascar. *Proc. Natl Acad. Sci. USA* **101**, 6045–6049.

Brown, K. A., S. E. Johnson, K. E. Parks, S. M. Holmes, T. Ivoandry, N. K. Abram, et al. 2013. Use of provisioning ecosystem services drives loss of functional traits across land use intensification gradients in tropical forests in Madagascar. *Biol. Cons.* **161**, 118–127.

Brown, K. A., K. E. Parks, C. A. Bethell, S. E. Johnson, and M. Mulligan. 2015. Predicting plant diversity patterns in Madagascar: understanding the effects of climate and land cover change in a biodiversity hotspot. *PLoS ONE* **10**, e0122721.

Burivalova, Z., M. R. Bauert, S. Hassold, N. T. Fatroandrianjafinonjasolomiovazo, and L. P. Koh. 2015. Relevance of global forest change data set to local conservation: case study of forest degradation in Masoala national park, Madagascar. *Biotropica*, **47**, 267–274.

Carter, S., M. Herold, V. Avitabile, S. B. Bruin, D. E. Veronique, L. Kooistra, et al. 2018. Agriculture-driven deforestation in the tropics from 1990–2015: emissions, trends and uncertainties. *Environ. Res. Lett.*, **13**, 014002.

Chazdon, R. L., E. N. Broadbent, D. M. A. Rozendaal, F. Bongers, A. M. A. Zambrano, T. M. Aide, et al. 2016. Carbon sequestration potential of second-growth forest regeneration in the Latin American tropics. *Sci. Adv.* **2**, e1501639.

Crowley, B. E. 2010. A refined chronology of prehistoric Madagascar and the demise of the megafauna. *Quatern. Sci. Rev.* **29**, 2591–2603.

Devries, B., J. Verbesselt, L. Kooistra, and M. Herold. 2015. Robust monitoring of small-scale forest disturbances in a tropical montane forest using Landsat time series. *Remote Sens. Environ.* **161**, 107–121.

Eckert, S., H. R. Ratsimba, L. O. Rakotondrasoa, L. G. Rajoelison, and A. Ehrensperger. 2011. Deforestation and forest degradation monitoring and assessment of biomass and carbon stock of lowland rainforest in the Analanjirofo region, Madagascar. *For. Ecol. Manage.* **262**, 1996–2007.

Elsa, M. O., P. A. Gregory, and F. L. Eric. 2017. Deforestation risk due to commodity crop expansion in sub-Saharan Africa. *Environ. Res. Lett.* **12**, 044015.

FAO. 2015. *Global forest resources assessment 2015*. UN Food and Agriculture Organisation, Rome.

Feldt, T., and E. Schlecht. 2016. Analysis of GPS trajectories to assess spatio-temporal differences in grazing patterns and land use preferences of domestic livestock in southwestern Madagascar. *Pastoralism* **6**, 5.

Fine, P. V., R. H. Ree, and R. J. Burnham. 2009. The disparity in tree species richness among tropical, temperate and boreal biomes: the geographic area and age hypothesis. Pp. 31–45 in R. P. Carson and S. A. Schnitzer, eds. *Tropical forest community ecology* Blackwell, London.

FRA. 2000. On Definitions of Forest and Forest change (No. Working Paper 33). Forestry Department, Food and Agriculture Organisation of the United Nations (FAO), Rome, Italy.

Gasparri, N. I., , T. Kuemmerle, P. Meyfroidt, Y. le Polain de Waroux and H. Kreft. 2016. The emerging soybean production frontier in Southern Africa: conservation challenges and the role of south-south telecouplings. *Conserv. Lett.*, **9**, 21–31.

Gautier, L., A. J. Tahinarivony, P. Ranirison, and S. Wohlhauser. 2018. Vegetation. Pp. 207–242 in S. M. Goodman, M. J. Raherilalao, S. Wohlhauser, eds. *The terrestrial protected areas of Madagascar: their history, description, and biota*. Association Vahatra, Antananarivo.

Ghazoul, J., Z. Burivalova, J. Garcia-Ulloa, and L. A. King. 2015. Conceptualizing forest degradation. *Trends Ecol. Evol.* **30**, 622–632.

Grinand, C., F. Rakotomalala, V. Gond, R. Vaudry, M. Bernoux, and G. Vieilledent. 2013. Estimating deforestation in tropical humid and dry forests in Madagascar from 2000 to 2010 using multi-date Landsat satellite images and the random forests classifier. *Remote Sens. Environ.* **139**, 68–80.

Hansen, M. C., S. V. Stehman, P. V. Potapov, T. R. Loveland, J. R. Townshend, R. S. Defries, et al. 2008. Humid tropical forest clearing from 2000 to 2005 quantified by using multitemporal and multiresolution remotely sensed data. *Proc. Natl Acad. Sci.* **105**, 9439–9444.

Hansen, M. C., S. V. Stehman, and P. V. Potapov. 2010. Quantification of global gross forest cover loss. *Proc. Natl Acad. Sci.* **107**, 8650–8655.

Hansen, M. C., P. V. Potapov, R. Moore, M. Hancher, S. A. Turubanova, A. Tyukavina, et al. 2013. High-resolution global maps of 21st-century forest cover change. *Science* **342**, 850–853.

Haque, M. I., and R. Basak. 2017. Land cover change detection using GIS and remote sensing techniques: a spatio-temporal study on Tanguar Haor, Sunamganj, Bangladesh. *Egypt. J. Remote Sens. Space Sci.* **20**, 251–263.

Harper, G. J., M. K. Steininger, C. J. Tucker, D. Juhn, and F. Hawkins. 2008. Fifty years of deforestation and forest fragmentation in Madagascar. *Environ. Conserv.* **34**, 325–333.

Harris, N. L., S. Brown, S. C. Hagen, S. S. Saatchi, S. Petrova, W. Salas, et al. 2012. Baseline map of carbon emissions from deforestation in tropical regions. *Science* **336**, 1573–1576.

Herold, M., R. M. Román-Cuesta, D. Mollicone, Y. Hirata, P. van Laake, G. P. Asner, et al. 2011. Options for monitoring and estimating historical carbon emissions from forest degradation in the context of REDD+. *Carbon Balance Manage.* **6**, 13.

Houghton, R. A., B. Byers, and A. A. Nassikas. 2015. A role for tropical forests in stabilizing atmospheric CO2. *Nat. Clim. Chang.* **5**, 1022.

Ingram, J. C., T. P. Dawson, and R. J. Whittaker. 2005. Mapping tropical forest structure in southeastern Madagascar using remote sensing and artificial neural networks. *Remote Sens. Environ.* **94**, 491–507.

Keenan, R. J., G. A. Reams, F. Achard, J. V. de Freitas, A. Grainger, and E. Lindquist. 2015. Dynamics of global forest area: results from the FAO Global Forest Resources Assessment 2015. *For. Ecol. Manage.* **352**, 9–20.

Kull, C. A. 2002a. The "Degraded" tapia woodlands of highland Madagascar: rural economy, fire ecology, and forest conservation. *J. Cult. Geogr.* **19**, 95–128.

Kull, C. A. 2002b. Madagascar's burning issue: the persistent conflict over fire. *Environ. Sci. Policy Sustain. Develop.*, **44**, 8–19.

Kull, C. A. 2012. Air photo evidence of historical land cover change in the highlands: wetlands and grasslands give way to crops and woodlots. *Madagascar Conserv. Develop.* **7**, 144–152.

Lambin, E. F., B. L. Turner, H. J. Geist, S. B. Agbola, A. Angelsen, J. W. Bruce, et al. 2001. The causes of land-use and land-cover change: moving beyond the myths. *Glob. Environ. Change* **11**, 261–269.

Lee, D. S., J. C. Storey, M. J. Choate, and D. Hayes. 2004. Four years of Landsat-7 on-orbit geometric calibration and performance. *IEEE Trans. Geosci. Remote Sens.* **42**, 2786–2795.

Martínez, P., R. Pérez, A. Plaza, P. Aguilar, M. Cantero, and J. Plaza. 2006. Endmember extraction algorithms from hyperspectral images. *Ann. Geophys.* **49**, 93–101.

Mcconnell, W. J., and C. A. Kull. 2014. Deforestation in Madagascar: debates over the island's forest cover and challenges of measuring forest change. Pp. 67–104 in I. R. Scales , eds. *Conservation and environmental management in Madagascar*. Routledge Taylor & Francis Group, London.

Moat, J., and P. Smith. 2007. *Atlas of the vegetation of Madagascar vegetation/Atlas de la vegetation de Madagascar (text in English and French)*. Royal Botanical Gardens, Kew.

Mora, F., V. J. Jaramillo, R. Bhaskar, M. Gavito, I. Siddique, J. E. K. Byrnes, et al. 2018. Carbon accumulation in Neotropical dry secondary forests: the roles of forest age and tree dominance and diversity. *Ecosystems* **21**, 536–550. https://doi.org/10.1007/s10021-017-0168-2.

Olofsson, P., G. M. Foody, M. Herold, S. V. Stehman, C. E. Woodcock, and M. A. Wulder. 2014. Good practices for estimating area and assessing accuracy of land change. *Remote Sens. Environ.* **148**, 42–57.

Paneque-Gálvez, J., J.-F. Mas, G. Moré, J. Cristóbal, M. Orta-Martínez, A. C. Luz, et al. 2013. Enhanced land use/cover classification of heterogeneous tropical landscapes using support vector machines and textural homogeneity. *Int. J. Appl. Earth Obs. Geoinf.* **23**, 372–383.

Phillips, O. L., and R. J. W. Brienen. 2017. Carbon uptake by mature Amazon forests has mitigated Amazon nations' carbon emissions. *Carbon Balance Manage.* **12**, 1.

Poorter, L., F. Bongers, T. M. Aide, A. M. A. Zambrano, P. Balvanera, J. M. Becknell, et al. 2016. Biomass resilience of Neotropical secondary forests. *Nature* **530**, 211–214.

Prestele, R., P. Alexander, M. D. A. Rounsevell, A. Arneth, K. Calvin, J. Doelman, et al. 2016. Hotspots of uncertainty in land-use and land-cover change projections: a global-scale model comparison. *Glob. Change Biol.* **22**, 3967–3983.

Quintano, C., A. Fernández-Manso, Y. E. Shimabukuro, and G. Pereira. 2012. Spectral unmixing. *Int. J. Remote Sens.* **33**, 5307–5340.

Rakotondrasoa, O. L., F. Malaisse, G. L. Rajoelison, T. M. Razafimanantsoa, M. R. Rabearisoa, B. S. Ramamonjisoa, et al. 2012. Tapia forest, endemic ecosystem to Madagascar: ecology, functions, causes of degradation and transformation: a review. *Biotechnol. Agron. Soc. Environ.* **16**, 541–552.

Scrieciu, S. S. 2007. Can economic causes of tropical deforestation be identified at a global level? *Ecol. Econ.* **62**, 603–612.

Stibig, H.-J., F. Achard, S. Carboni, R. Raši, and J. Miettinen. 2014. Change in tropical forest cover of Southeast Asia from 1990 to 2010. *Biogeosciences* **11**, 247–258.

United Nations Framework Convention on Climate Change (UNFCCC). 2018. Report of the technical assessment of the proposed forest reference emission level of Madagascar submitted in 2018. Available at https://redd.unfccc.int/submissions.html?country=mdg

Vågen, T.-G. 2006. Remote sensing of complex land use change trajectories – a case study from the highlands of Madagascar. *Agr. Ecosyst. Environ.* **115**, 219–228.

Vermote, E. F., D. Tanre, J. L. Deuze, M. Herman, and J. J. Morcette. 1997. Second simulation of the satellite signal in the solar spectrum, 6S: an overview. *IEEE Trans. Geosci. Remote Sens.* **35**, 675–686.

Vieilledent, G., C. Grinand, and R. Vaudry. 2013. Forecasting deforestation and carbon emissions in tropical developing countries facing demographic expansion: a case study in Madagascar. *Ecol. Evol.* **3**, 1702–1716.

Waeber, P., L. Wilmé, B. Ramamonjisoa, C. Garcia, D. Rakotomalala, Z. Rabemananjara, et al. 2015. Dry forests in Madagascar: neglected and under pressure. *Int. Forest Rev.* **17**, 127–148.

Whitmore, T. C. 1998. *An Introduction to Tropical Rainforests*. Oxford University Press, New York, NY.

Zaehringer, J. G., S. Eckert, and P. Messerli. 2015. Revealing Regional Deforestation Dynamics in North-Eastern Madagascar – Insights from multi-temporal land cover change analysis. *Land* **4**, 454–474.

Zahawi, R. A., J. P. Dandois, K. D. Holl, D. Nadwodny, J. L. Reid, and E. C. Ellis. 2015. Using lightweight unmanned aerial vehicles to monitor tropical forest recovery. *Biol. Cons.* **186**, 287–295.

Zinner, D., C. Wygoda, L. Razafimanantsoa, R. Rasoloarison, H. T. Andrianandrasana, J. U. Ganzhorn, et al. 2014. Analysis of deforestation patterns in the central Menabe, Madagascar, between 1973 and 2010. *Reg. Environ. Change* **14**, 157–166.

Supporting Information

Additional supporting information may be found online in the Supporting Information section at the end of the article.

Figure S1. Accuracy assessment maps of sub-pixel analysis mapped as root mean square errors each pixel. The errors indicate difference between modelled end-members and images in three periods (*c.* 2014, 2002 and 1994). Differences ranged from *c.* 1–7% representing regions of low and high variations respectively. Background image is shaded relief of Madagascar.

Figure S2. Validating the distribution of deforestation and forest degradation as determined from sub-pixel analysis with Hansen et al. (2013) global forest cover datasets. Areas of agreement during first interval are represented as red (84 242 ha) while during second interval are represented as blue (32 381 ha).

Figure S3. Map showing the dominant transitions from the perspective of forest loss during first *(left-side) and* second *(right-side)* intervals in medium altitude moist evergreen forest. Inset figure shows the geographical

range of medium altitude moist evergreen forest in Madagascar.

Figure S4. Map showing the dominant transitions from the perspective of forest loss during first (*left-side) and* second *(right-side)* intervals in lowland evergreen moist forest. Inset figure shows the geographical range of lowland evergreen moist forest in Madagascar.

Figure S5. Map showing dominant transitions from the perspective of forest gain during first (*left-side) and* second *(right-side)* intervals in dry deciduous forest and scelrophyllous woodland. Inset figure shows the geographical range of dry deciduous forest and scelrophyllous woodland in Madagascar.

